Quantum Electronics **45** (6) 556–560 (2015)

INTERFEROMETRY

PACS numbers: 42.25.Hz; 42.25.Kb; 42.30.Wb
DOI: 10.1070/QE2015v045n06ABEH015616

Chromatic dispersion effects in ultra-low coherence interferometry

V.V. Lychagov, V.P. Ryabukho

Abstract. **We consider the properties of an interference signal shift from zero-path-difference position in the presence of an uncompensated dispersive layer in one of the interferometer arms. It is experimentally shown that in using an ultra-low coherence light source, the formation of the interference signal is also determined by the group velocity dispersion, which results in a nonlinear dependence of the position of the interference signal on the geometrical thickness of the dispersive layer. The discrepancy in the dispersive layer and compensator refractive indices in the third decimal place is experimentally shown to lead to an interference signal shift that is an order of magnitude greater than the pulse width.**

Keywords: *white-light interferometry, dispersion, full-field optical coherence tomography, coherence.*

1. Introduction

The methods of optical imaging of the internal structure of layered and scattering objects, built on the principles of low-coherence interferometry [1, 2], have been increasingly widely used in recent years. The role of the impulse response (or the point scattering function) in these systems is played by a pulse in the interference signal from radiation probing an object: the duration of this pulse determines the spatial resolution of the method, and the pulse position in time indicates the optical distance to an object or to an inhomogeneity in its structure. The interference signal from the object with a complex internal structure consists of a set of such pulses, each of which corresponds to an optical inhomogeneity or an interface between two media inside the object. Under real conditions the listed properties can be violated to a varying degree.

The duration of the interference pulse is determined by the coherence time of probe radiation, depending on the width of its frequency spectrum: the wider the spectrum of the light source, the shorter the interference pulse and the higher the spatial resolution of the system. On the basis of these considerations, a new method, namely full-field optical coherence tomography, or interference microscopy [3, 4], has been proposed. This method relies on the use of a source with a very broad emission spectrum – a thermal white-light source such as an incandescent lamp, which has made it possible to obtain an extremely short (~1 μm) interference pulse. However, the use of broadband radiation entails a number of problems. In particular, the longitudinal correlation properties of probe radiation are affected not only by the emission spectrum, but also by the angular spectrum of the field produced by an extended source, which can lead to a number of effects, discussed in [5–9].

As a result of a significant impact of spectral properties of the object itself and optical scheme elements, the effective emission spectrum differs significantly from the original spectrum of radiation entering the interferometer [10, 11]. In these studies Kalyanov et al. [10, 11] considered the amplitude modulation of the probe radiation spectrum. However, not only the amplitude but also the phase of the spectral components of radiation can change. The reason for the phase modulation is the dispersion of the refractive index of the object and the optical elements of the interferometer. The dispersion of the refractive index leads to the fact that monochromatic components of broadband radiation propagate different optical paths in media having the same geometric thickness. This can cause a number of effects in interferometry [12–14]: a broadening of the interference pulse, an emergence of the interference pulse frequency modulation and a change in the interference pulse shape, a reduction of the contrast of interference fringes, and an occurrence of beatings in the signal when superimposing several interference pulses. Obviously, the wider the emission spectrum, the more pronounced the effects. Manifestation of dispersion effects in white-light interference microscopy was considered in [15, 16]. Despite a rather complete description of the resulting effects [15], an important issue on the position of the interference pulse in the recorded signal was not given sufficient attention. For example, Denielmeyer and Weber [13] indicate that the position of the pulse envelope is determined by the group velocity dispersion (GVD) of the uncompensated layer of the medium. However, it follows from the GVD definition that it can be also characterised by the spectral dependence. At the same time, the accuracy with which it is possible to determine the position of the interference pulse in the signal is a key metrological characteristic of optical imaging.

In this paper, the chromatic dispersion effects for ultra-low coherence interferometry are studied by the example of a scanning Michelson interferometer [17, 18], the scheme of which forms the basis of many measurement systems, including coherence tomography and interference microscopy systems. We consider two variants of interference experiments – numerical calculations of the interference signal and an experiment with a real interferometer. A simple idea is used as the basis for the experiments. In changing the optical path differ-

V.V. Lychagov N.G. Chernyshevsky Saratov State University, ul. Astrakhanskaya 83, 410012 Saratov, Russia; e-mail: cepes@yandex.ru;
V.P. Ryabukho N.G. Chernyshevsky Saratov State University, ul. Astrakhanskaya 83, 410012 Saratov, Russia; Institute of Precision Mechanics and Control, Russian Academy of Sciences, ul. Rabochaya 24, 410028 Saratov, Russia; e-mail: rvp-optics@yandex.ru

Received 7 July 2014; revision received 11 August 2014
Kvantovaya Elektronika **45** (6) 556–560 (2015)
Translated by I.A. Ulitkin

ence, in the scanning interferometer a pulse signal is formed whose envelope has a maximum value when the path difference is equal to zero. If a layer of a dispersive medium is introduced into one of the interferometer arms, the maximum of the interference pulse will shift from the zero-path-difference position by some value. It is believed that the value of this shift is determined by the optical thickness of the introduced layer, which in turn is determined by the GVD of the layer. In other words, if a virtual compensator with the same geometrical thickness but a fixed refractive index equal to the GVD of the layer is introduced into the second arm of the interferometer, the interference pulse must shift back to the position corresponding to the zero path difference.

2. Numerical calculation of the interference signal

The scheme of the numerical experiment is as follows. A transparent plate having a geometric thickness d and a phase refractive index $n(k)$, where k is the wavenumber, is introduced into one arm of the scanning Michelson interferometer. In the other arm of the interferometer we introduce a compensator having the same thickness d and some refractive index n_0, which is independent of k. As a result, for each spectral component of the interfering waves at the interferometer output we can introduce an additional path difference, which depends on the refractive index of the plate,

$$\Delta l_0(k) = 2d(n(k) - n_0) \tag{1}$$

and, accordingly, an additional phase difference

$$\Delta\varphi_0(k) = k\Delta l_0(k). \tag{2}$$

The purpose of the numerical experiment is that for each value of the geometric thickness d of the layer, we find a refractive index n_0, at which there is no shift of the maximum of the interference pulse envelope on the scale of the path difference.

It is convenient to employ in calculations the representation of the interference signal $I(\Delta)$ using the complex Fourier transform [19]

$$I(\Delta) \sim \int_{k_1}^{k_2} S(k)\exp(-\mathrm{i}k\Delta)\,\mathrm{d}k\,, \tag{3}$$

where $S(k)$ is the spatial frequency spectrum of the interfering radiation; $[k_1, k_2]$ is the domain of $S(k)$ definition; and Δ is the optical path difference. If the thicknesses d of the dispersive layer and the compensator are nonzero, then each spectral component undergoes an additional phase shift $\Delta\varphi_0(k)$, which must be taken into account in calculating the resulting interference signal by introducing additional phase modulation of the original spectrum [19]

$$I(\Delta) \sim \int_{k_1}^{k_2} \tilde{S}(k)\exp(-\mathrm{i}k\Delta)\,\mathrm{d}k\,, \tag{4}$$

where

$$\tilde{S}(k) = S(k)\exp[\mathrm{i}\Delta\varphi_0(k)]. \tag{5}$$

For the calculations it is necessary to determine the spectrum of the interfering radiation $S(k)$, which will take into account the parameters of radiation and optical elements, close to a real interference experiment. The cumulative effect of the spectral characteristics of these elements determines the effective spectrum of the interfering radiation [10, 11]. In a real interference experiment, the results of which are discussed below, we used an incandescent lamp with a tungsten filament. Propagating in the interferometer the light of this lamp passed twice through a 15-mm-thick plane-parallel plate made of BK7 glass and a 25 mm cube beam splitter also made of BK7 glass. The interference signal was measured using a Ge photodetector. Figure 1 shows the spectral characteristics of each of these elements [20] and the resulting effective emission spectrum. The dispersion curve $n(k)$ of BK7 glass was calculated using the Sellmeier equation with the coefficients borrowed from [21].

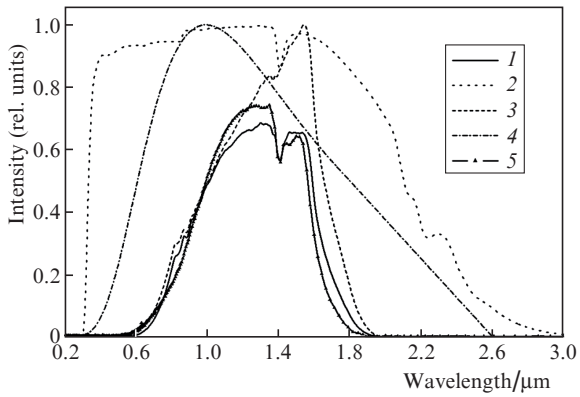

Figure 1. (*1*) Transmission spectrum of 80-mm-thick BK7 glass, (*2*) spectral sensitivity of a germanium photodetector, (*3*) emission spectrum of a tungsten lamp and (*4*) resultant and (*5*) experimentally measured effective spectra.

The interference pulse was calculated for several values of the geometrical thickness d (from 0 to 3.4 mm) of the dispersive layer and for several values of the refractive index n_0 (from 1.5195 to 1.5225). For each pair of values of d and n_0 we determined the position of the maximum of the interference pulse envelope, $\Delta_{\max}$. The dependence $\Delta_{\max}(d, n_0)$ is conveniently represented in the form of a contour map (Fig. 2).

From the results of the calculation we can draw two conclusions. Firstly, for various geometric dispersive-layer thicknesses d, the compensator's refractive index n_0, at which the maximum of the interference pulse envelope is at the zero-path-difference position, will be different (the zero contour line in the contour map corresponds to this conclusion). Secondly, at larger thicknesses d (from 1 mm or greater) the dependence of the pulse position on the refractive index n_0 becomes strong. In changing n_0 in the third decimal place the shift of the interference pulse can be from 2 μm (which is comparable to the width of the pulse) to 15 μm.

3. Interference experiment

In a real interference experiment it is quite difficult to accurately implement the scheme of the numerical experiment. To solve this problem, we inserted two plane-parallel BK7 glass plates with the geometrical thickness 15620 ± 1 and 15750 ± 1 μm in the interferometer arms. The thinner plate was installed in one of the interferometer arms on a rotating platform by means of

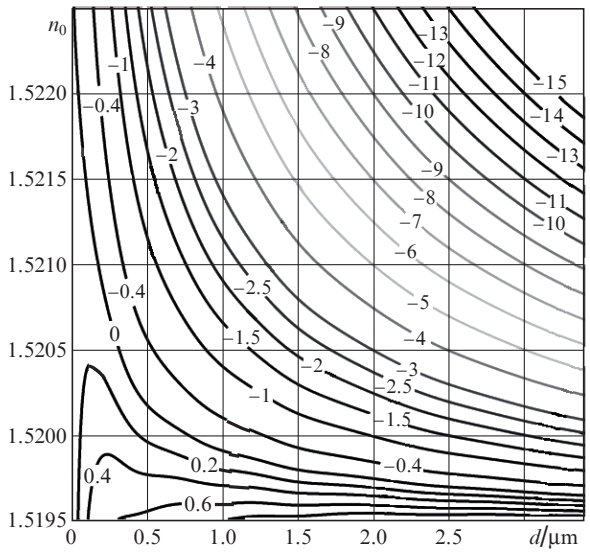

Figure 2. Dependence of the position of the envelope maximum Δ_{max} (in μm) on the thickness d of the dispersive layer and the refractive index n_0 of the compensator.

which it was rotated with a step 30′ (accuracy 3′). Thus, we changed the thickness of the uncompensated dispersive layer, through which one of the interfering waves passes. The disadvantage of this approach is that due to refraction at the inclined plate the geometric path of each spectral component also depends on the refractive index. The other plate was mounted in the second arm of the interferometer to compensate for the thickness of the first plate.

Figure 3 shows the variation in the geometric path length of the wave in the dispersive layer as a function of the angle of the plate rotation.

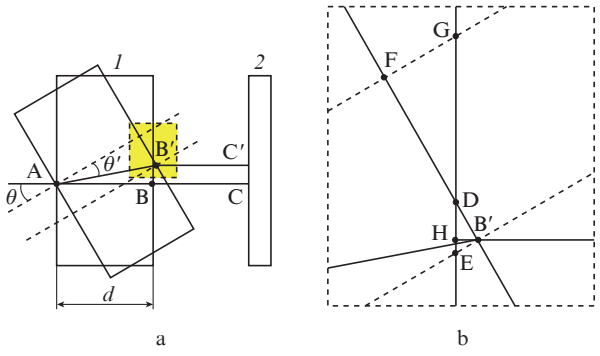

Figure 3. Scheme for calculating the dispersive layer thickness [(*1*) plane-parallel glass plate, (*2*) mirror, (θ) plate rotation angle].

For the rotation angle $\theta = 0$, the optical path that the light travels from point A to the mirror and back is $l_1 = 2(\mathrm{AB}n(k) + \mathrm{BC})$. By turning the plate through the angle θ, the optical path of the same beam is $l_2 = 2(\mathrm{AB}'n(k) + \mathrm{B}'\mathrm{C}')$. It follows from the calculation that

$$\mathrm{AB}' = \frac{d}{\cos\theta'}, \tag{6}$$

where $d = \mathrm{AB}$ is the plate thickness.

Thus, the dependence of the increment of the dispersive layer thickness on the rotation angle of the plate can be calculated by the formula

$$\Delta d = \frac{d}{\cos\theta'} - d\,. \tag{7}$$

The optical path increment $\Delta l = l_2 - l_1$, as follows from Fig. 3, is

$$\Delta l = 2\left[\frac{dn(k)}{\cos\theta'} - dn(k) - \mathrm{HB}'\right]. \tag{8}$$

It can be shown that the segment $\mathrm{FB}' = d\tan\theta'$, and the segment $\mathrm{FG} = d(1 - \cos\theta)/\cos\theta$. Then, from the triangles DFG and DHB′ we can find that

$$\mathrm{HB}' = d(\tan\theta'\sin\theta - 1 + \cos\theta). \tag{9}$$

Figure 4 shows the dependences of the optical path increment Δl on the rotation angle of the plate for two wavelengths and the difference between these increments.

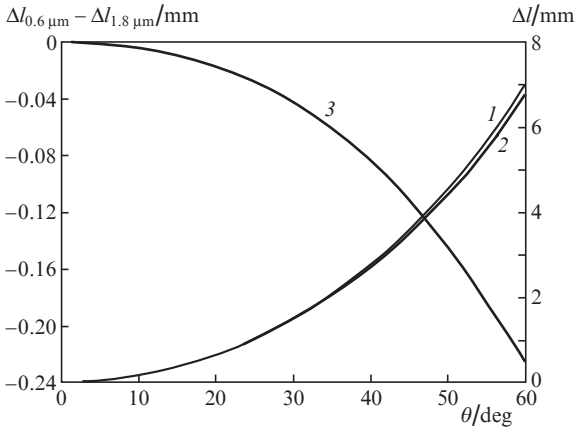

Figure 4. Optical path increments Δl at (*1*) $n = 1.497$, $\lambda = 1.8$ μm and (*2*) $n = 1.516$, $\lambda = 0.6$ μm and (*3*) the difference of these increments as a function of the plate rotation angle θ.

With the scheme described we recorded a series of interference pulses at different angles of rotation of the plate. Figure 5 shows an example of two pulses, one of which corresponds to an almost zero thickness of the dispersive layer, and the second – to its maximum thickness, i.e., the maximum rotation of the plate.

It is impossible to provide an interference experiment with a compensator having a wavelength-independent refractive index n_0. Therefore, the optical path difference Δl, resulting from the rotation the plate, and the corresponding interference pulse displacement Δl_d were compensated by calculations. The displacement of the maximum of the interference pulse envelope, Δl_d, was measured experimentally and the compensating shift Δl_c was calculated by formula (8) and (9) in which $n(k)$ was replaced by n_0. Thus one can find the experimental dependence of the position of the maximum of the interference pulse envelope on the rotation angle of the plate (thickness of the dispersive layer) and the refractive index n_0 of the virtual compensator:

$$\Delta_{max}^{exp}(\theta, n_0) = \Delta l_d - \Delta l_c\,. \tag{10}$$

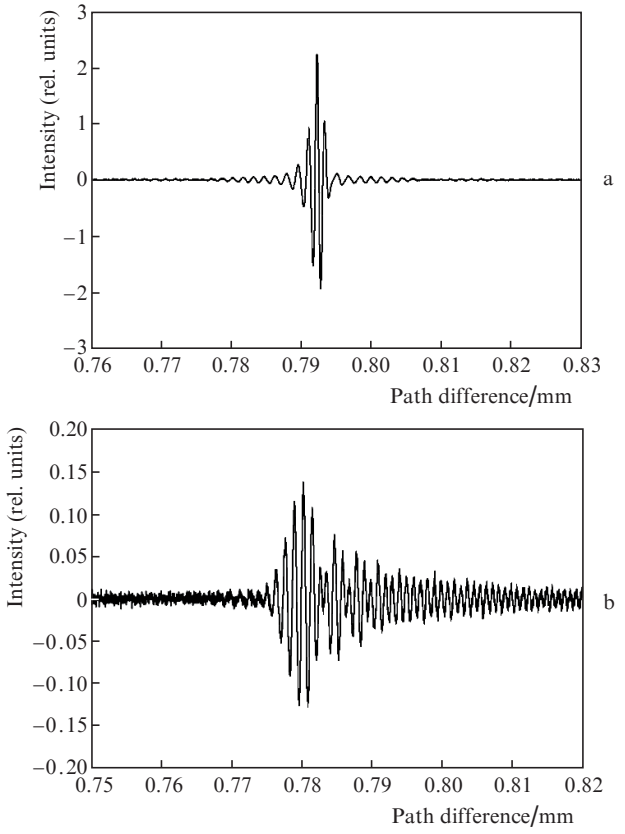

Figure 5. Experimental interference pulses obtained at (a) minimal and (b) maximal thicknesses of the dispersive layer.

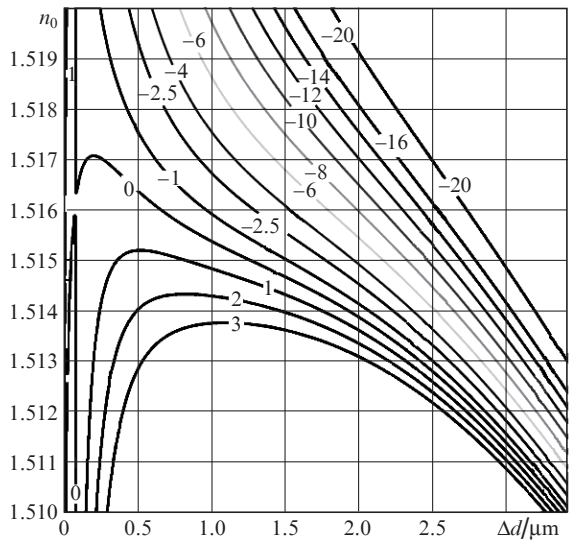

Figure 6. Dependence of the position of the experimental interference pulse envelope maximum $\Delta_{\max}^{\exp}$ (in μm) on the thickness Δd of the dispersive layer and the refractive index n_0 of the compensator.

To compare the experimental results with numerical calculations, it is necessary to know the thickness of the dispersive layer, Δd. But the wavelength dependence of Δd does not allow one to unambiguously assign some single value Δd to the rotation angle of the plate. For illustrative purposes, the layer thickness Δd can be estimated for some average refractive index from the interval of n_0 values. In addition, before calculating $\Delta_{\max}^{\exp}(\Delta d, n_0)$ the experimental dependence of the maximum of the interference pulse envelope on the rotation angle Δl_d of the plate was interpolated by a higher-order polynomial function. Figure 6 shows the corresponding contour map illustrating the dependence of the maximum of the experimental interference pulse envelope on the thickness of the dispersive layer and the refractive index of the compensator.

Comparison of Figs 2 and 6 leads to the conclusion about the fundamental agreement of numerical results and experimental measurements. Existing differences in the shapes of contours can be explained by differences in the methods of creating a dispersive layer in numerical and real experiments. The numerical experiment allows one to calculate a pure dependence of dispersion effects on the geometrical thickness of the layer, whereas the scheme with a rotary plate is one of the few variants for creating a dispersive layer of variable thickness in real interference experiments.

4. Conclusions

The results presented in Figs 2 and 6 lead to an important conclusion. The position of the interference pulse is governed by a refractive index n_0, which is dependent on the dispersive layer thickness d. Obviously, at different geometrical thicknesses d the mutual phase delay of individual spectral components of broadband light, resulting from the passage through this layer, will be different. When using broadband light, as was done in this study, GVD starts exerting a significant influence on the formation of an interference pulse. This leads not only to a lengthening of the interference pulse and a change in its shape, as noted in many papers, but also to a complicated dependence of the pulse shift on the dispersive layer thickness (see Figs 2 and 6). For $d = 1$ mm the change in the compensator's refractive index n_0 by 0.002 causes a displacement of the interference pulse by no more than 3 μm. Increasing the thickness of the dispersive layer up to 3 mm for the same parameters of the compensator results in the displacement of the interference pulse by 15 μm. The minimum (in the absence of dispersion) pulse width at half-magnitude of the interference pulse in the above experiment was about 2 μm.

In practical terms, this means that in studying the structure of a dispersive medium with a white-light interferometer, the spatial resolution not only decreases due to the lengthening of the pulse (see Fig. 6), but also the position of this pulse and, therefore, the position of the inhomogeneity in an object to which the pulse corresponds become ambiguous. This casts doubt on the accuracy of the image of internal optical structure of an object obtained using this type of system.

Another problem that arises from the ambiguity of the position of the interference pulse is related to the method for determining the refractive index of the material by the known optical and geometrical thicknesses. Obviously, inaccurate determination of the pulse position leads to an error in evaluating the optical thickness of the object.

The object can be sufficiently thin. In this case, as seen from Figs 2 and 6, the shift of the pulse is much smaller than its width and can be neglected. However, in the optical scheme of the interferometer an uncompensated dispersive layer can be present. To eliminate the dispersion effects use is made of the compensators, having known dispersive properties that are similar to the properties of a medium. However, the contour lines in Figs 2 and 6 suggest that even a small deviation

of the dispersion curve of the compensator from the dispersion curve of the test sample leads to a pulse shift. It should also be noted that all the results were obtained for the BK7 grade glass, which has relatively weak dispersion, whereas in samples of other materials the effect may be more pronounced.

Acknowledgements. The study was partially supported by the Leading Scientific Schools Programme (Grant No. 703.2014.2).

References

1. Drexler W., Fujimoto J.G. *Optical Coherence Tomography. Technology and Application* (Berlin–Heidelberg–New York: Springer, 2008).
2. Nolte D.D. *Optical Interferometry for Biology and Medicine* (New York–Dordrecht–Heidelberg–London: Springer, 2012).
3. Dubois A., Grieve K., Moneron G., Lecaque R., Vabre L., Boccara C. *Appl. Opt*., **43**, 2874 (2004).
4. Dubois A., Vabre L., Boccara C., Beaurepaire E. *Appl. Opt*., **41**, 805 (2002).
5. Lyakin D.V., Ryabukho V.P. *Kvantovaya Elektron*., **43**, 949 (2013) [*Quantum Electron*., **43**, 949 (2013)].
6. Ryabukho V.P., Lyakin D.V., Grebenyuk A.A., Klykov S.S. *J. Opt.*, **15**, 025405 (2013).
7. Grebenyuk A.A., Ryabukho, V.P. *Proc. SPIE Int. Soc. Opt. Eng*., **8427**, 84271M (2012).
8. Abdulhalim I. *Annalen der Physik*, **524**, 787 (2012).
9. Zeylikovich I. *Appl. Opt*., **47**, 2171 (2008).
10. Kalyanov A.L., Lychagov V.V., Smirnov I.V., Ryabukho V.P. *Opt. Spektrosk*., **115**, 207 (2013).
11. Kalyanov A.L., Lychagov V.V., Ryabukho V.P., Smirnov I.V. *J. Opt*., **14**, 125708 (2012).
12. Hitzenberger C.K., Baumgartner A., Fercher A.F. *Opt. Commun*., **154**, 179 (1998).
13. Danielmeyer H.G., Weber H.P. *Phys. Rev. A*, **3**, 1708 (1971).
14. De Groot P. *Opt. Lett*., **17**, 898 (1992).
15. Pavlicek P., Soubusta J. *Appl. Opt*., **43**, 766 (2004).
16. Pfortner A., Schwider J. *Appl. Opt*., **40**, 6223 (2001).
17. Steel W.H. *Progress in Optics*, **5**, 145 (1966).
18. Malacara D. *Optical Shop Testing* (Hoboken, New Jersey: John Wiley & Sons Inc., 2007).
19. Bell R.J. *Introductory Fourier Transform Spectroscopy* (New York: Acad. Press, 1972; Moscow: Mir, 1975).
20. http://www.thorlabs.com.
21. Schott Optical Glass - Collection Datasheets. http://www.schott.com.